processes

MDPI

Article

Parametric Study of Wire-EDM Process in Al-Mg-MoS_2 Composite Using NSGA-II and MOPSO Algorithms

Vladimir Modrak [1,*], Ranjitharamasamy Sudhakara Pandian [2] and Shanmugakani Senthil Kumar [3]

[1] Department of Industrial Engineering and Informatics, Faculty of Manufacturing Technologies, Technical University of Kosice, 080 01 Prešov, Slovakia
[2] Department of Manufacturing Engineering, School of Mechanical Engineering, Vellore Institute of Technology, Vellore 632014, Tamil Nadu, India; sudhame@gmail.com
[3] Department of Mechanical Engineering, Sri Vidya College of Engineering & Technology, Affiliated to Anna University, Chennai 626005, Tamil Nadu, India; 2020rsp@gmail.com
* Correspondence: vladimir.modrak@tuke.sk

Abstract: Al-Mg-based composite is used in producing a variety of components. To improve the machinability of the composite, MoS_2 is added. For characterizing the machining of the Al-Mg-based composite, different wt.% (2, 4, and 6) of MoS_2 are added as reinforcement. Wire Electrical Discharge Machining (WEDM) process is performed to analyze the kerf width and surface roughness. Due to the complex nature of the WEDM process, the necessity for its optimization through the use of innovative methods is well-proven in the process of research. Evolutionary algorithms, specifically genetic algorithm based on NSGA-II and Multiple Objective Particle Swarm Optimization (MOPSO), are used for optimizing kerf width and surface roughness. For assessing the impact of current, pulse on time, and gap voltage on kerf width and surface roughness, an analysis of the selected WEDM process parameters is performed. MOPSO takes lesser iterations as compared to NSGA-II in giving nearly the same optimal fronts for achieving low kerf width and surface roughness. The 10–12 A of current, 50–57 µs of pulse on time, and 30–33 V of gap voltage are used for the WEDM process based on the Pareto-optimal solutions and better performance is achieved on the samples. In addition, the supplementary DOE method is applied to determine the relationship between factors affecting a process and the response. The analysis revealed that current has played a major part in the governance of kerf width and surface roughness over pulse on time and gap voltage for Al-Mg-MoS_2 composite.

Keywords: wire-EDM; NSGA-II; MOPSO; pulse on time; gap voltage

Citation: Modrak, V.; Pandian, R.S.; Kumar, S.S. Parametric Study of Wire-EDM Process in Al-Mg-MoS_2 Composite Using NSGA-II and MOPSO Algorithms. *Processes* **2021**, *9*, 469. https://doi.org/10.3390/pr9030469

Academic Editor: Tizazu Mekonnen

Received: 24 January 2021
Accepted: 25 February 2021
Published: 5 March 2021

1. Introduction

There is a great demand for machine components with better strength to weight ratio, improved resistance shown towards corrosion, and wear and tear in the automotive sector. For example, Al-Mg composite is the solution to problems related to low corrosion resistance and high strength of tank car bodies [1]. Moreover, aluminum metal matrix composite is considered as a possible substitute for traditional materials in the shipping and aerospace industries, electronic products, and industrial machinery [2]. Al-Mg composite plays a major role because of its machinability properties, such as good specific strengths, specific stiffness, specific moduli, and fewer coefficients of linear expansion properties [3,4]. To improve the machinability of Al-Mg composite, MoS_2 is added to the composite by the ball-milling process. Al-Mg-MoS_2 composite thus reduces wear loss, protects the components from corrosion, and also improves the machining properties by making it an excellent composite material to be used in the automotive sector. To analyze the properties of Al-Mg-MoS_2 composite, different wt.% of MoS_2 are added. Wire Electric Discharge Machining (WEDM) is used for machining the composite to have less tool wear and also to get low residual stresses. Moreover, WEDM is used for high cutting speed and high

precision works for enhancing productivity and accuracy to manufacture press tools, molds, prototype parts, and complicated shapes, etc. [5]. WEDM does not require high cutting forces for the removal of material with complex profiles. Hence, it is used for the machining of Al-Mg-MoS_2 composite with varied wt.% of MoS_2.

2. Related Works

Fard et al. [6] reported the impact of current, pulse off and pulse on time, gap voltage, and tension of wire on surface texture in Al–SiC composite. Pulse on time and discharge current have an effect on both cutting velocity and surface roughness of Al–SiC composite. Mahanta et al. [7] studied B4C and fly ash reinforced Al 7075 alloy for sustainable production. It was found that current and pulse-on-time affect all three measures: Power consumption, material removal rate, and surface finish. Ahsan Ali Khan et al. [8] examined the influence of peak current, wire-speed, and wire diameter on the WEDM process in mild steel. An increase in pulse peak current and a reduction in wire speed have contributed towards deprived surface integrity on the workpiece. Ming et al. [9] found that while optimizing the WEDM parameters in YG15, surface quality decreases with the rise of pulse-on time. Zhang et al. [10] confirmed that the surface quality of the workpiece decreases with the increase in pulse-on time while machining SKD11 steel.

Sonawane et al. [11] used Taguchi's L27 orthogonal arrangement to study how pulse-off time interval, pulse-on period, discharge voltage, discharge current, wire feed speed, and cable tension influenced kerf width and surface roughness while machining an intricate profile on Ti-6Al-4V. Scanning Electron Microscopy investigation of the parts machined has proved that an increase in pulse on time and discharge current results in the deterioration of the surface due to the presence of deep craters, globules of debris, voids, and micro cracks. Himanshu Payal et al. [12] attempted an amalgam methodology of Taguchi, GRA, and PCA to optimize the machining parameters involved in the die-sinking EDM process.

Deb et al. [13] introduced a new algorithm NSGA-II, an improved version of NSGA to overcome computational complexity, non-elitism approach. NSGA-II was used to optimize the WEDM process in Ti 6-2-4-2 alloy [14], AISI 5160 steel [15], high-speed steel [16], AISI D3 tool steel [17,18]. Somashekhar et al. [19] calculated the significant parameters like material removal rate, overcut, and surface roughness in Micro-WEDM of aluminum by simulated annealing (SA) optimization. A maximum overcut value of around 69 μ was observed at discharge energy of 2,645 μJ.

Coello and Lechuga [20] introduced a novel method, MOPSO (Multiple Objective Particle Swarm Optimization) for finding the Pareto-optimal fronts. Kumar et al. [21] disclosed an improvement of surface roughness from 2.689 to 2.448 μm by using MOPSO optimization for Inconel 825. Saffaran et al. [22] used MOPSO and simulated annealing to optimize the EDM process of AISI2312 and found the results were within ±7% error. MOPSO converged quicker than simulated annealing. However, the optimized values were approximately the same. Similarly, MOPSO algorithm was used for the optimization of WEDM process of stainless steel of SS304 grade [23] and Inconel 718 [24]. An investigation on the tribological performance of Al-4%Mg added with MoS_2 was offered by Kumar et al. [25]. They found out, e.g., that tested samples are exceptionally plowed from the softer pin surface to the hard asperity of the counter disc material, and hence, wear loss is amplified. The influence of WEDM parameters for surface finish and cutting speed for the Ni-based super alloy through multi-parametric optimization was investigated by Kumar and Dhanabalan [26], where the WEDM process parameters for Inconel-600 has been optimized by Grey relational method coupled with Taguchi method. According to Vundavilli et al. [27], WEDM is a complex process, and thus it is difficult to determine a unique set of optimal combinations of cutting parameters. In this nexus, a multi-parameter complexity analysis can be employed to demonstrate how variables are mutually intercorrelated [28,29].

In this work, non-linear regression is applied for modelling the WEDM process parameters. L27 orthogonal array Box–Behnken design matrix is used to conduct the

WEDM process. For the optimization of the WEDM process, the metaheuristics algorithms, NSGA-II and MOPSO, are employed. The metaheuristics were selected since they are suitable for a wide range of problems and allow identifying the best decision options [30]. The results derived from these algorithms are compared, and confirmation tests have been conducted for validation.

3. Design of Real-Time Experiments

Wire Electrical Discharge Machining is an unconventional method of machining, where a traveling wire chips off the material in a controlled manner. Both the workpiece and wire are submerged in a dielectric liquid while machining. The cutting debris of the process is flushed away along with the dielectric. WEDM is mainly used for its high precision cutting of electrically conductive materials. WEDM does not damage or compromise the finished product. Hence, there is no need for additional thermal treatments after machining. To have minimal residual stress on the workpiece material, WEDM is chosen over other non-conventional machining techniques. Figure 1 shows the procedural steps involved in real-time experiments.

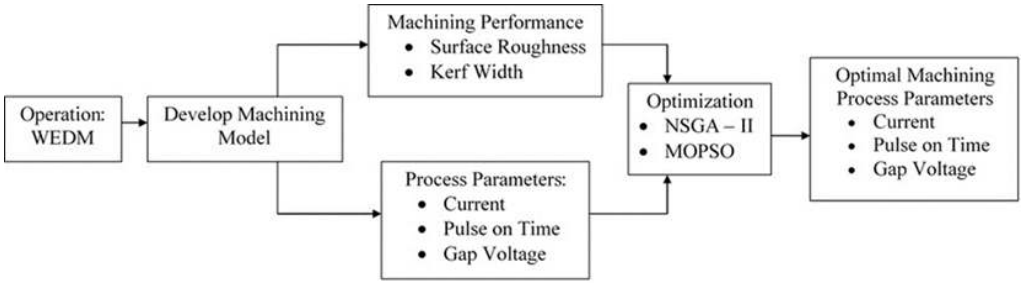

Figure 1. An approach to machining process optimization.

The experiments are carried out using the Excetek V650 manufacturer machine. The electrode material used in the experiments is a copper-zinc (Cu-Zn) wire with a diameter of 0.25 mm. Deionized water is used as the dielectric medium to machine the workpieces like pure Al, Al-4%Mg alloy, Al-4%Mg-2%MoS_2, Al-4%Mg-4%MoS_2, and Al-4%Mg-6%MoS_2 composite. All five workpieces were prepared through the powder metallurgy route. Table 1 shows the various control factors involved in the WEDM process.

Table 1. Wire Electrical Discharge Machining (WEDM) parameters and its levels.

Control Factors	Unit	Symbol	Range	Level 1	Level 2	Level 3
Current	A	I	9–15	9	12	15
Pulse on Time	µs	Ton	50–100	50	75	100
Gap Voltage	V	V	30–40	30	35	40

An L27 orthogonal arrangement table is employed for the WEDM process on all five samples during the intricate manufacturing process. This approach uses a design of orthogonal arrays by combining the complete parameter space with only a small number of experiments. This tool is quite frequently applied for optimizing the experimental conditions for maximizing/minimizing any target output. Through this method, it is often possible to greatly improve process performance and reduce waste. In every process, a precise description and distinction of the processes are required for quality control and process improvement [31].

The relation between the process parameters: Current, pulse on time, and gap voltage, and their impact on the quality measures as well as kerf width and surface roughness is obtained using regression. The regression equation is of the form [7]:

$$Y = b_0 + \text{Sum}\{I = 1..3\}b_i \times x_i + \text{Sum}\{I = 1..3\}b_{ii} \times x_i\text{^}2 + \text{Sum}\{I = 1..2\}(\text{Sum}\{j = i+1..3\}b_{ij} \times x_i \times x_j), \quad (1)$$

where b_0 is constant and all b_i's, b_{ii}'s, and b_{ij}'s are regression coefficients. Y holds linear, squared and product terms of x_i. The regression coefficients are obtained using Python programming. The regression equations for all the five samples are listed below:

Sample 1: Pure Aluminum

$$y(1) = 0.33529 + 0.0046824 \times x(1) - 0.00080307 \times x(2) - 0.0037791 \times x(3) + 1.9713 \times 10^{-05} \times x(1) \times x(2) + 2.7815 \times 10^{-05} \times x(1) \times x(3) + 1.0314 \times 10^{-05} \times x(2) \times x(3) - 0.00022776 \times x(1)\hat{}2 - 4.0445 \times 10^{-06} \times x(2)\hat{}2 + 4.8094 \times 10^{-05} \times (3)\hat{}2 \quad (2)$$

$$y(2) = 8.186 + 0.013343 \times x(1) + 0.00024252 \times x(2) - 0.2565 \times x(3) - 0.00027087 \times x(1) \times x(2) + 0.00039991 \times x(1) \times x(3) + 0.00045118 \times x(2) \times x(3) + 0.0010694 \times x(1)\hat{}2\ 1.9824 \times 10^{-05} \times x(2)\hat{}2 + 0.003215 \times x(3)\hat{}2; \quad (3)$$

Sample 2: Al-4%Mg

$$y(1) = 0.31336 - 0.011655 \times x(1) - 0.00050156 \times x(2) + 0.0025289 \times x(3) + 1.8476 \times 10^{-05} \times x(1) \times x(2) + 4.1994 \times 10^{-05} \times x(1) \times x(3) + 7.496 \times 10^{-06} \times x(2) \times x(3) + 0.00042499 \times x(1)\hat{}2 + 2.6703 \times 10^{-06} \times x(2)\hat{}2 - 4.5244 \times 10^{-05} \times x(3)\hat{}2; \quad (4)$$

$$y(2) = 3.531 + 0.06966 \times x(1) - 0.003446 \times x(2) + 0.038242 \times x(3) + 0.00023891 \times x(1) \times x(2) - 0.00018854 \times x(1) \times x(3) - 8.7165 \times 10^{-06} \times x(2) \times x(3) - 0.0028926 \times x(1)\hat{}2 + 1.7735 \times 10^{-05} \times x(2)\hat{}2 - 0.00043418 \times x(3)\hat{}2; \quad (5)$$

Sample 3: Al-4%Mg-2%MoS2

$$y(1) = 0.33946 - 0.0096184 \times x(1) - 0.00095392 \times x(2) + 0.001257 \times x(3) + 5.6949 \times 10^{-05} \times x(1) \times x(2) + 0.00010234 \times x(1) \times x(3) + 4.2289 \times 10^{-06} \times x(2) \times x(3) + 0.00013301 \times x(1)\hat{}2 + 3.0439 \times 10^{-06} \times x(2)\hat{}2 - 3.2943 \times 10^{-05} \times x(3)\hat{}2; \quad (6)$$

$$y(2) = 0.44212 + 0.051265 \times x(1) + 0.02432 \times x(2) + 0.17335 \times x(3) + 0.00031832 \times x(1) \times x(2) - 2.5547 \times 10^{-05} \times x(1) \times x(3) - 0.00020219 \times x(2) \times x(3) - 0.0021158 \times x(1)\hat{}2 - 4.8464 \times 10^{-05} \times x(2)\hat{}2 - 0.001933 \times x(3)\hat{}2; \quad (7)$$

Sample 4: Al-4%Mg-4%MoS2

$$y(1) = 0.22955 - 0.0074107 \times x(1) + 0.00070705 \times x(2) + 0.0034004 \times x(3) + 1.3495 \times 10^{-05} \times x(1). \times x(2) + 3.169 \times 10^{-05} \times x(1) \times x(3) - 7.3971 \times 10^{-06} \times x(2) \times x(3) + 0.00025402 \times x(1)\hat{}2 - 2.2262 \times 10^{-06} \times x(2)\hat{}2 - 3.7712 \times 10^{-05} \times x(3)\hat{}2; \quad (8)$$

$$y(2) = 5.6231 - 0.049497 \times x(1) - 0.00077891 \times x(2) + 0.026841 \times x(3) + 0.00012845 \times x(1) \times x(2) + 0.00018508 \times x(1) \times x(3) - 7.0711 \times 10^{-06} \times x(2) \times x(3) + 0.0014015 \times x(1)\hat{}2 + 8.7106 \times 10^{-06} \times x(2)\hat{}2 - 0.000 \times 36523 \times x(3)\hat{}2; \quad (9)$$

Sample 5: Al-4%Mg-6%MoS2

$$y(1) = 0.2625 - 0.0067164 \times x(1) + 0.0001755 \times x(2) + 0.0024636 \times x(3) + 2.1966 \times 10^{-05} \times x(1). \times x(2) + 1.0433 \times 10^{-06} \times x(1) \times x(3) + 1.4677 \times 10^{-06} \times x(2) \times x(3) + 0.00024191 \times x(1)\hat{}2 - 1.6296 \times 10^{-06} \times x(2)\hat{}2 - 2.9184 \times 10^{-05} \times x(3)\hat{}2; \quad (10)$$

$$y(2) = 3.4833 - 0.045099 \times x(1) + 0.0079706 \times x(2) + 0.15972 \times x(3) - 0.00060826 \times x(1) \times x(2) - 0.00043229 \times x(1) \times x(3) - 1.3229 \times 10^{-05} \times x(2) \times x(3) + 0.0043558 \times x(1)\hat{}2 + 1.5639 \times 10^{-05} \times x(2)\hat{}2 - 0.0021558 \times x(3)\hat{}2; \quad (11)$$

where, y(1) represents kerf width, y(2) represents surface roughness, x(1) defines current, x(2) defines pulse on time, and x(3) defines gap voltage.

The regressed values obtained using the above equations for surface roughness and kerf width have a mean R2 value around 1 for all the workpieces.

4. Multi-Objective Optimization of the Process Parameters

When the manufacturer wants to design a product with minimum fabrication cost, then there arises a need to find the optimal solutions to avoid wastage of material, labor cost, time, and money. Hence, WEDM process parameters have to be optimized. No single combination of process parameters will offer the least kerf width besides the least surface roughness at the same time. To sort out this issue, NSGA-II and MOPSO are utilized for obtaining Pareto-optimal solutions.

4.1. Non-Dominated Sorting Generic Algorithm-II (NSGA-II)

Non-dominated Sorting Genetic Algorithm-II (NSGA-II) is an improved version of NSGA, which includes elitist and crowding tactics. Elitism is proved to be a pre-requisite for the convergence to true Pareto front in Multi-Objective Optimization. Tournament selection is used to diversify among non-dominated solutions. For each iteration in NSGA-II, non-dominated solutions that are identified in the population are correlated with an external set of non-dominated solutions found in the entire search process. Thus, NSGA-II gives an improved feast of results and an improved convergence nearer to a true Pareto-optimal front.

The procedure for NSGA-II is given below:

Step 1: Initialize the population (N = 20) based on the bounding values of the input parameters;

Step 2: Calculate fitness functions (kerf width and surface roughness) for every individual;

Step 3: Group the initialized population in terms of the non-dominated sorting;

Step 4: Select the individuals based on crowding distance and ranking and then perform cross-over operation with the factor of 0.95 and mutation operations with the factor of 0.01 to generate offspring;

Step 5: Combine the population of parents and offspring and find the individuals for the next generation based on the ranking and crowding distance;

Step 6: If maximum generation (500) is reached, then stop, otherwise go to Step 4.

The flowchart for NSGA-II is shown in Figure 2.

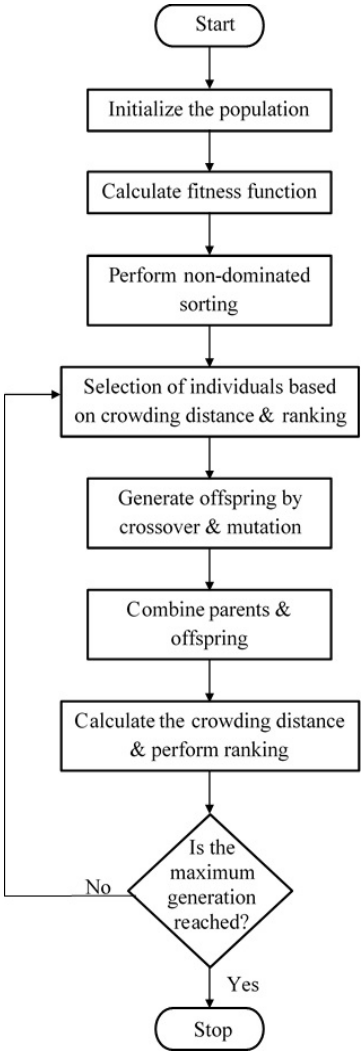

Figure 2. Flowchart for Non-dominated Sorting Genetic Algorithm-II (NSGA-II).

4.2. Multi-Objective Particle Swarm Optimization (MOPSO)

Particle Swarm Optimization (PSO) is enthused from the choreography of bird flocks. Multi-Objective Particle Swarm Optimization (MOPSO) is particularly suitable for multi-objective optimization, typically due to its high speed of convergence, like that of single-objective optimization.

MOPSO Algorithm used is given below:

Step 1: Initialize the population (collection of particles) by randomly selecting an n-dimensional array with array elements to have uniform probability within the bounding limits. Initialize the position and speed of each particle;

Step 2: Evaluate the fitness functions (kerf width and surface roughness) for each particle;

Step 3: Search for non-dominated solutions and store them in an external repository;

Step 4: For each particle, set the current position of the particle as the local best and form a non-dominated local set. Individuals with better crowding distance are preferred to maintain diversity;

Step 5: Update the particle velocity and position and evaluate the fitness functions. Expand and update the non-dominated global and local solutions by removing the dominated solutions from the set. Find the local best and global best for each particle;

Step 6: If stopping criteria are not met, update the weight and move to Step 4 or else stop.

The flowchart for MOPSO is shown in Figure 3.

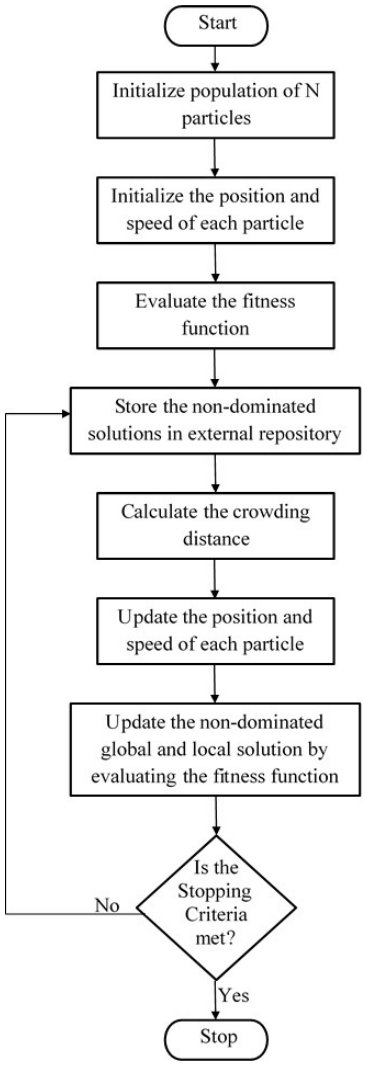

Figure 3. Flowchart for Multiple Objective Particle Swarm Optimization (MOPSO).

5. Results and Discussion

For the WEDM process of Al-Mg-MoS_2 composite, the L27 orthogonal array Box–Behnken design matrix is used. Kerf width and surface roughness are measured for each WEDM process. These measures are tabulated in Table 2.

Table 2. Experimental Results of WEDM process.

Sl. No	Current	Pulse on Time	Gap Voltage	Kerf Width (mm)					Surface Roughness (μm)				
				Pure Al	Al-4% Mg	Al-4% Mg-2% MoS_2	Al-4% Mg-4% MoS_2	Al-4% Mg-6% MoS_2	Pure Al	Al-4% Mg	Al-4% Mg-2% MoS_2	Al-4% Mg-4% MoS_2	Al-4% Mg-6% MoS_2
1.	9	50	30	0.2913	0.2904	0.2895	0.2830	0.2873	4.0109	4.5758	5.1802	5.8281	6.3337
2.	9	50	35	0.2937	0.2928	0.2919	0.2907	0.2897	4.1157	4.6641	5.3466	5.8872	6.3603
3.	9	50	40	0.2947	0.2894	0.2928	0.2916	0.2906	4.2179	4.6396	5.4287	5.8758	6.3630
4.	9	75	30	0.2971	0.2962	0.2953	0.2940	0.2930	4.3282	4.5931	5.5450	5.9053	6.3777
5.	9	75	35	0.2916	0.2979	0.2995	0.2957	0.2947	4.4347	4.6526	5.5975	5.8981	6.4271
6.	9	75	40	0.3029	0.3013	0.2920	0.2979	0.2969	4.5559	4.6299	5.6466	5.8869	6.4371
7.	9	100	30	0.3043	0.3044	0.2959	0.2993	0.2922	4.6398	4.6895	5.8082	5.9198	6.4274
8.	9	100	35	0.3095	0.3095	0.2986	0.3003	0.3002	4.7404	4.6799	5.8777	5.9266	6.9193
9.	9	100	40	0.3128	0.3103	0.3029	0.3013	0.3010	4.8539	4.7314	6.0268	5.9522	6.4440
10.	12	50	30	0.2941	0.2903	0.2894	0.2818	0.2820	4.9263	4.6399	5.1205	5.8176	6.3426
11.	12	50	35	0.2955	0.2929	0.2892	0.2907	0.2898	4.1279	4.6929	5.2394	5.8400	6.3869
12.	12	50	40	0.2984	0.2934	0.2925	0.2913	0.2903	4.2280	4.7097	5.4383	5.8536	6.3607
13.	12	75	30	0.3029	0.2959	0.2950	0.2937	0.2927	4.5278	4.6910	5.5588	5.8699	6.4295
14.	12	75	35	0.3046	0.2975	0.2966	0.2954	0.2944	4.4211	4.7357	5.7998	5.8895	6.3919
15.	12	75	40	0.3091	0.2962	0.2999	0.2974	0.2964	4.3009	4.7488	5.9013	5.9023	6.4703
16.	12	100	30	0.3129	0.3062	0.3061	0.2994	0.2983	4.6191	4.7142	5.9438	5.9148	6.4377
17.	12	100	35	0.3194	0.3093	0.3073	0.3012	0.3002	4.7209	4.6909	6.0787	5.9287	6.3987
18.	12	100	40	0.3245	0.3138	0.3103	0.3042	0.3029	4.8214	4.7792	6.1816	5.9568	6.4832
19.	15	50	30	0.2974	0.2930	0.2899	0.2871	0.2877	4.1372	4.6291	5.2603	5.8353	6.3520
20.	15	50	35	0.2995	0.2963	0.2927	0.2915	0.2905	4.2205	4.6710	5.4328	5.8526	6.4692
21.	15	50	40	0.3019	0.2987	0.2960	0.2947	0.2937	4.5224	4.6575	5.5069	5.8652	6.4229
22.	15	75	30	0.3039	0.3039	0.2946	0.2982	0.2972	4.7247	4.6917	5.6391	5.8593	6.4864
23.	15	75	35	0.3073	0.3093	0.3029	0.3017	0.2997	4.6261	4.7068	5.7382	5.9093	6.4514
24.	15	75	40	0.3147	0.3103	0.3063	0.3029	0.3010	4.9062	4.7299	5.9032	5.8956	6.4065
25.	15	100	30	0.3176	0.3155	0.3129	0.3030	0.3029	4.7549	4.7673	5.9317	5.9379	6.4694
26.	15	100	35	0.3208	0.3197	0.3196	0.3071	0.3053	4.8617	4.8173	6.3271	5.9717	6.4554
27.	15	100	40	0.3251	0.3210	0.3206	0.3109	0.3093	4.9091	4.8093	5.9849	5.9665	6.5058

Kerf width and surface roughness must be as low as possible in machining. Because of the conflicting nature of the performance measures, NSGA-II and MOPSO algorithms are used to find the optimal machining parameters for each workpiece. These algorithms are implemented in python. Initially, the population size of 20 is considered for all the samples in NSGA-II and MOPSO.

For pure Al sample, the following Figure 4 shows the Pareto optimal solutions found by NSGA-II and MOPSO.

Pareto optimal solutions obtained show that kerf width and surface roughness of pure Al is low for a current of 9 A and gap on a voltage of 33 V. With these conditions, when pulse on time is increased, kerf width increases and surface roughness decreases. For Al-4%Mg sample, Figure 5a,b shows the Pareto optimal solutions obtained by NSGA-II and MOPSO.

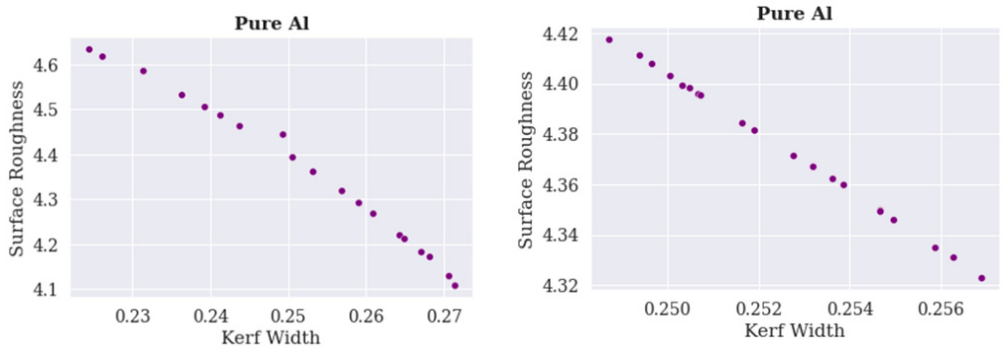

(**a**) (**b**)

Figure 4. Pareto optimal solutions of Pure Al by (**a**) NSGA-II and (**b**) MOPSO.

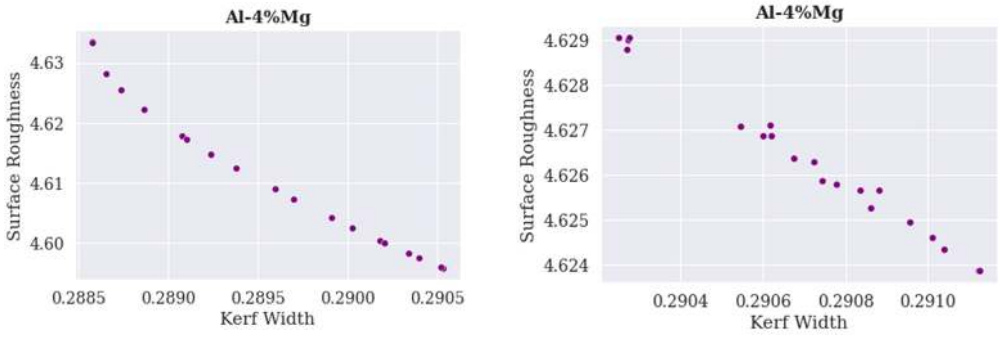

(**a**) (**b**)

Figure 5. Pareto optimal solutions for Al-4%Mg by (**a**) NSGA-II, and (**b**) MOPSO.

For Al-4%Mg sample, kerf width and surface roughness are low when 9–10 A current, 50 µs of pulse on time, and 30–32 V of gap voltage according to the Pareto-optimal solutions. For Al-4%Mg-2%MoS_2 sample, Figure 6a,b shows the Pareto optimal solutions obtained by NSGA-II and MOPSO algorithms.

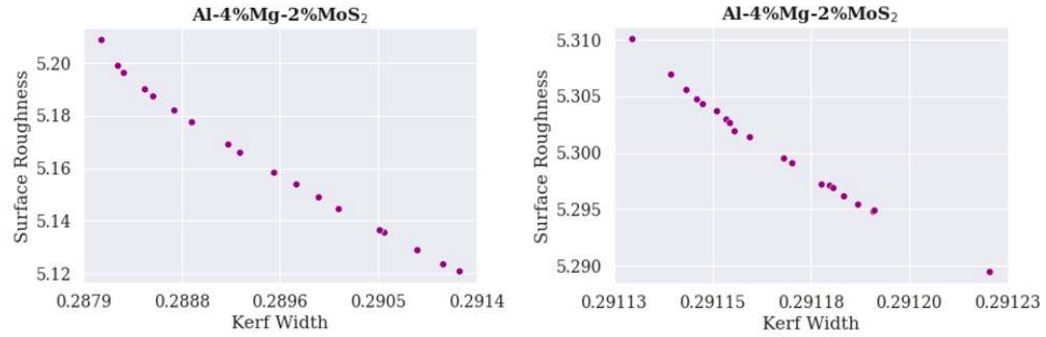

(**a**) (**b**)

Figure 6. Pareto optimal solutions for Al-4%Mg-2%MoS_2 by (**a**) NSGA-II, and (**b**) MOPSO.

For Al-4%Mg-2%MoS_2, Pareto-optimal solutions are obtained at 10 A of peak current, 50 µs of pulse on time, and 30–33 V of gap voltage. For Al-4%Mg-4%MoS_2 sample, Figure 7a,b shows the Pareto optimal solutions obtained by NSGA-II an MOPSO algorithms.

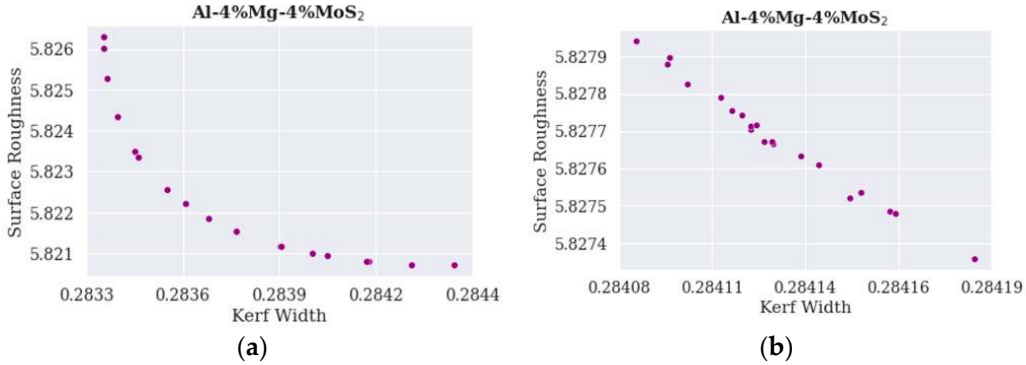

Figure 7. Pareto optimal solutions for Al-4%Mg-4%MoS_2 by (**a**) NSGA-II, and (**b**) MOPSO.

For the Al-4%Mg-4%MoS_2 sample, Pareto-optimal solutions are obtained at 11–12 A of peak current, 50 µs of pulse on time, and 30 V of gap voltage.

For Al-4%Mg-6%MoS_2 sample, Figure 8a,b shows the Pareto optimal solutions obtained by NSGA-II and MOPSO algorithms. For the Al-4%Mg-6%MoS_2 sample, NSGA-II provides Pareto-optimal solutions for 10–11 A current, a pulse on time of 50 µs, and a gap voltage of 30 V. MOPSO provides Pareto-optimal solutions for 10 A current, pulse on time of 57 µs, and gap voltage of 31 V.

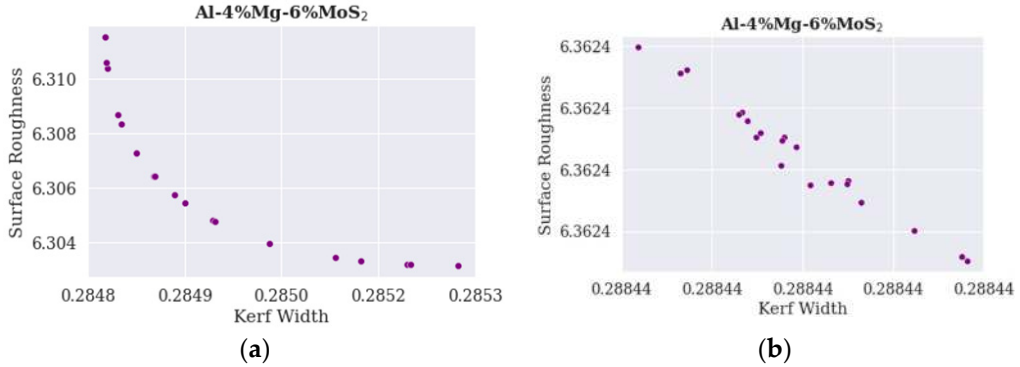

Figure 8. Pareto optimal solutions for Al-4%Mg-6%MoS_2 by (**a**) NSGA-II, and (**b**) MOPSO.

By employing the optimization algorithms, the following optimal machining parameters were identified, as shown in Tables 3 and 4.

From Tables 3 and 4, it is evident that samples other than pure Al have low kerf width and surface roughness, for about 9–12 A current, 50 µs pulse on time, and gap voltage of 30–33 V. For pure Al, optimal solutions have been obtained for 9 A current, pulse on time around 75 µs, and gap voltage of 33 V. Hence, we infer that upon adding Mg and MoS_2, the pulse on time can be reduced to obtain proper finishing of the samples. Because, as the pulse on time and current increases, a large volume of heat energy is released during machining, which results in deep craters, debris, voids, and micro-cracks, thereby deteriorating the surface finish.

Both NSGA-II and MOPSO have provided almost the same range of machining parameters for low values of kerf width and surface roughness for the different composite materials. MOPSO takes lesser than 10 iterations to converge towards the Pareto-optimal solutions. However, NSGA-II takes 200–400 iterations to converge to the Pareto-optimal solutions. Hence, for this optimization of the WEDM process, MOPSO is much more efficient than NSGA-II because of its lesser computation time.

Table 3. Machining parameters range obtained using NSGA-II.

Sample	Kerf Width	Surface Roughness	Current	Pulse on Time	Gap Voltage
Pure Al	0.251 ± 0.014	4.364 ± 0.160	9	72.970 ± 15.742	33.069 ± 1.545
Al-4%Mg	0.2895	4.611 ± 0.012	9.793 ± 0.666	50	30
Al-4%Mg-2%MoS_2	0.289 ± 0.001	5.159 ± 0.027	10.746 ± 1.400	50	30
Al-4%Mg-4%MoS_2	0.283	5.822 ± 0.001	12.413 ± 0.640	50	30
Al-4%Mg-6%MoS_2	0.284	6.306 ± 0.002	10.914 ± 0.441	50	30

Table 4. Machining parameters range obtained using MOPSO.

Sample	Kerf Width	Surface Roughness	Current	Pulse on Time	Gap Voltage
Pure Al	0.252 ± 0.002	4.374 ± 0.028	9.106 ± 0.007	73.454 ± 2.603	33.244 ± 0.410
Al-4%Mg	0.291	4.626 ± 0.001	9.552 ± 0.155	50.232 ± 0.069	32.016 ± 0.182
Al-4%Mg-2%MoS_2	0.291	5.300 ± 0.004	10.463 ± 0.079	50.497 ± 0.134	33.314 ± 0.031
Al-4%Mg-4%MoS_2	0.284	5.827	11.901 ± 0.045	50.126 ± 0.019	30.563 ± 0.001
Al-4%Mg-6%MoS_2	0.288	6.362	10.573	57.644 ± 0.001	31.732

6. Validation of Predicted Results

To verify the results obtained from MOPSO and NSGA-II, the confirmatory experiments are performed on the MoS_2-reinforced Al-4%Mg samples, and the outcomes of the same are represented and compared in Table 5.

Table 5. Comparison of Predicted and Confirmatory test results.

Factors/Samples	Predicted Value			Confirmatory Test Value		
	Al-4%Mg-2%MoS_2	Al-4%Mg-4%MoS_2	Al-4%Mg-6%MoS_2	Al-4%Mg-2%MoS_2	Al-4%Mg-4%MoS_2	Al-4%Mg-6%MoS_2
Current (A)	10	12	10	10	12	10
Pulse on time (µs)	50	50	57	50	50	57
Gap voltage (V)	33	30	31	33	30	31
Kerf width (mm)	0.291	0.284	0.288	0.289	0.284	0.289
Surface roughness (µm)	5.289	5.827	6.362	5.294	5.825	6.359

Table 5 shows the confirmatory test results performed after optimization of the WEDM parameters. It is found that confirmatory test values are almost nearer to the predicted values as found through optimization using MOPSO. Thus, the optimized values can be used to obtain the desired kerf width and surface roughness for the WEDM process.

7. Conclusions

Multi-objective optimization of process parameters of WEDM in the machining of Al-Mg-MoS_2 composite with varied wt. % of MoS_2 using the Box–Behnken designs is performed in this article. The kerf width and surface roughness were studied as a function of process parameters. Both NSGA-II and MOPSO are used for finding the keys to the declared problems. From the obtained results of the experiments, and analysis of WEDM process parameters it can be noted that:

- MOPSO takes lesser than 10 iterations to optimize the WEDM for each sample when compared to NSGA-II, which takes more than 200 iterations for each sample. Moreover, MOPSO takes lesser computing time when compared with NSGA-II to produce the optimal values.

- For Al-Mg-MoS_2 composite, current around 10–12 A, pulse on time of about 50–57 µs, and gap voltage of 30–33 V can produce the required optimal solutions for kerf width and surface roughness.
- Confirmatory tests also prove the validity of the solutions obtained through the optimization algorithms.

Hence, the developed model can be effectively used to predict kerf width and surface roughness for Al-Mg-MoS_2 composite. As regards further research, the presented design of experiments by utilizing NSGA-II and MOPSO may be in the future extended to optimize, e.g., tribological properties.

As Al-Mg composites possess both the properties of resistance to corrosion and wear, most of the automation industries are interested in developing and replacing the existing Al-based composites with Al-Mg composites in automotive parts. Therefore, more parts will be designated to produce, leading to mass sensing of automated production lines with a very high data stream. Thus, the Industry 4.0 based production lines and the processes carried out on them react badly to forcing parameter settings, significantly deviating from stable process settings [32]. DOE methodology, when implemented in Industry 4.0, will need to face challenges, such as large data streams, large data sets, large data dimensions, non-Gaussian data distributions, and non-linear relationships between controlled factors.

Author Contributions: Writing-original draft preparation has been done by V.M. Conceptualization and methodology were performed by all the authors. Writing-review has been done by R.S.P. Experimentation has been carried out by S.S.K. Results investigations were analyzed and evaluated by R.S.P. All authors have read and agreed to the published version of the manuscript.

Funding: The authors would like to thank the Ministry of Education, Science, Research and Sport of the Slovak Republic for the financial support of this work by grant KEGA, project No. 025TUKE-4/2020.

Institutional Review Board Statement: Not applicable.

Informed Consent Statement: Not applicable.

Data Availability Statement: The study did not report any data.

Conflicts of Interest: The authors herewith declare that they have no conflict of interest to the publication of this article.

References

1. Yang, G.; Fu, D.; Li, Q.; Liu, Z. A finite element analysis on mechanical behavior of Al/Al-Mg composites for the design of tank cars under actual measuring loads. *Eng. Fail. Anal.* **2019**, *103*, 294–307. [CrossRef]
2. Shahid, R.N.; Scudino, S. Microstructure and Mechanical Behavior of Al-Mg Composites Synthesized by Reactive Sintering. *Metals* **2018**, *8*, 762. [CrossRef]
3. Jiang, J.; Xiao, G.; Che, C.; Wang, Y. Microstructure, mechanical properties and wear behavior of the rheoformed 2024 alu-minum matrix composite component reinforced by Al2O3 nanoparticles. *Metals* **2018**, *8*, 460. [CrossRef]
4. Zhang, P.-X.; Yan, H.; Liu, W.; Zou, X.-L.; Tang, B.-B. Effect of T6 Heat Treatment on Microstructure and Hardness of Nanosized Al2O3 Reinforced 7075 Aluminum Matrix Composites. *Metals* **2019**, *9*, 44. [CrossRef]
5. Kant, G.; Sangwan, K.S. Prediction and optimization of machining parameters for minimizing power consumption and surface roughness in machining. *J. Clean. Prod.* **2014**, *83*, 151–164. [CrossRef]
6. Fard, R.K.; Afza, R.A.; Teimouri, R. Experimental investigation, intelligent modeling and multi-characteristics optimization of dry WEDM process of Al–SiC metal matrix composite. *J. Manuf. Process.* **2013**, *15*, 483–494. [CrossRef]
7. Mahanta, S.; Chandrasekaran, M.; Samanta, S.; Arunachalam, R.M. EDM investigation of Al 7075 alloy reinforced with B4C and fly ash nanoparticles and parametric optimization for sustainable production. *J. Braz. Soc. Mech. Sci. Eng.* **2018**, *40*, 263. [CrossRef]
8. Khan, A.A. Relationship of Surface Roughness with Current and Voltage During Wire EDM. *J. Appl. Sci.* **2006**, *6*, 2317–2320. [CrossRef]
9. Ming, W.; Zhang, Z.; Zhang, G.; Huang, Y.; Guo, J.; Chen, Y. Multi-Objective Optimization of 3D-Surface Topography of Machining YG15 in WEDM. *Mater. Manuf. Process.* **2014**, *29*, 514–525. [CrossRef]

10. Zhang, G.; Zhang, Z.; Ming, W.; Guo, J.; Huang, Y.; Shao, X. The multi-objective optimization of medium-speed WEDM process parameters for machining SKD11 steel by the hybrid method of RSM and NSGA-II. *Int. J. Adv. Manuf. Technol.* **2014**, *70*, 2097–2109. [CrossRef]
11. Sonawane, S.A.; Ronge, B.P.; Pawar, P.M. Multi-characteristic optimization of WEDM for Ti-6Al-4V by applying grey relational investigation during profile machining. *J. Mech. Eng. Sci.* **2019**, *13*, 6059–6087. [CrossRef]
12. Payal, H.; Maheshwari, S.; Bharti, P.S. Parametric optimization of EDM process for Inconel 825 using GRA and PCA approach. *J. Inf. Optim. Sci.* **2019**, *40*, 291–307. [CrossRef]
13. Deb, K.; Pratap, A.; Agarwal, S.; Meyarivan, T. A fast and elitist multiobjective genetic algorithm: NSGA-II. *IEEE Trans. Evolut. Comput.* **2002**, *6*, 182–197. [CrossRef]
14. Garg, M.P.; Jain, A.; Bhushan, G. Modelling and multi-objective optimization of process parameters of wire electrical discharge machining using non-dominated sorting genetic algorithm-II. *Proc. Inst. Mech. Eng. Part B J. Eng. Manuf.* **2012**, *226*, 1986–2001. [CrossRef]
15. Khullar, V.R.; Sharma, N.; Kishore, S.; Sharma, R. RSM- and NSGA-II-Based Multiple Performance Characteristics Optimization of EDM Parameters for AISI 5160. *Arab. J. Sci. Eng.* **2017**, *42*, 1917–1928. [CrossRef]
16. Kumar, K.; Agarwal, S. Multi-objective parametric optimization on machining with wire electric discharge machining. *Int. J. Adv. Manuf. Technol.* **2012**, *62*, 617–633. [CrossRef]
17. Krishnan, S.A.; Samuel, G.L. Multi-objective optimization of material removal rate and surface roughness in wire electrical discharge turning. *Int. J. Adv. Manuf. Technol.* **2012**, *67*, 2021–2032. [CrossRef]
18. Golshan, A.; Gohari, S.; Ayob, A. Modeling and optimization of cylindrical wire electro discharge machining of AISI D3 tool steel using non-dominated sorting genetic algorithm. In Proceedings of the 2011 International Conference on Graphic and Image Processing, Cairo, Egypt, 1–2 October 2011.
19. Somashekhar, K.P.; Mathew, J.; Ramachandran, N. A feasibility approach by simulated annealing on optimization of micro-wire electric discharge machining parameters. *Int. J. Adv. Manuf. Technol.* **2012**, *61*, 1209–1213. [CrossRef]
20. Coello, C.C.; Lechuga, M. MOPSO: A proposal for multiple objective particle swarm optimization. In Proceedings of the Proceedings of the 2002 Congress on Evolutionary Computation. CEC'02 (Cat. No.02TH8600), Honolulu, HI, USA, 12–17 May 2002; Volume 2, pp. 1051–1056. [CrossRef]
21. Kumar, P.; Gupta, M.; Kunar, V. Multi-Objective Particle Swarm Optimization of WEDM Process Parameters for Inconel 825. *J. Comput. Appl. Res. Mech. Eng.* **2019**, in press. [CrossRef]
22. Saffaran, A.; Moghaddam, M.A.; Kolahan, F. Optimization of backpropagation neural network-based models in EDM process using particle swarm optimization and simulated annealing algorithms. *J. Braz. Soc. Mech. Sci. Eng.* **2020**, *42*, 1–14. [CrossRef]
23. Nguyen, T.T.; Dang, X.P.; Nguyen, T.A.; Trinh, Q.H. Experiments and optimization for the WEDM process: A trade-off analysis between surface quality and production rate. *Vietnam. J. Mech.* **2020**, *42*, 105–121. [CrossRef]
24. Mohanty, C.P.; Mahapatra, S.S.; Singh, M.R. An intelligent approach to optimize the EDM process parameters using utility concept and QPSO algorithm. *Eng. Sci. Technol. Int. J.* **2017**, *20*, 552–562. [CrossRef]
25. Kumar, S.S.; Pandian, R.S.; Pitchipoo, P. A study on tribological behavior of Al-4%Mg incorporated with MoS2. *Mater. Res. Express* **2020**, *7*, 016578. [CrossRef]
26. Kumar, S.; Dhanabalan, S. Influence of WEDM parameters on surface roughness and cutting speed for NI-based super alloy and multi-parametric optimization using Taguchi and grey relational analysis. *Int. J. Ethics Eng. Manag. Educ.* **2018**, *5*, 7–13.
27. Vundavilli, P.R.; Kumar, J.P.; Priyatham, C.S. Parameter optimization of wire electric discharge machining pro-cess using GA and PSO. In Proceedings of the IEEE-International Conference on Advances in Engineering, Science and Management (ICAESM-2012), Nagapattinam, India, 30–31 March 2012; pp. 180–185.
28. Modrák, V.; Marton, D.; Kulpa, W.; Hricova, R. Unraveling complexity in assembly supply chain networks. In Proceedings of the 2012 4th IEEE International Symposium on Logistics and Industrial Informatics, Smolenice, Slovakia, 5–7 September 2012; pp. 151–156.
29. Aghighi, M.; Backstrom, C. A multi-parameter complexity analysis of cost-optimal and net-benefit planning. In Proceedings of the 26th International Conference on Automated Planning and Scheduling, London, UK, 12–17 June 2016; Volume 26.
30. Dima, I.C.; Gabrara, J.; Pachura, P. Using the expert systems in the operational management of production. In Proceedings of the 11th WSEAS international conference on mathematics and computers in business and economics and 11th WSEAS international conference on Biology and chemistry, Iasi, Romania, 13–15 June 2010; pp. 307–312.
31. Kumar, A.; Motwani, J.; Otero, L. An application of Taguchi's robust experimental design technique to improve service performance. *Int. J. Qual. Reliab. Manag.* **1996**, *13*, 85–98. [CrossRef]
32. Mazumdar, S.; Hoa, S. Application of Taguchi method for process enhancement of on-line consolidation technique. *Composites* **1995**, *26*, 669–673. [CrossRef]